Value Added Hydrocarbons from Distilled Tall Oil via Hydrotreating over a Commercial NiMo Catalyst

DATASET *in* INDUSTRIAL & ENGINEERING CHEMISTRY RESEARCH · JULY 2013

Impact Factor: 2.59 · DOI: 10.1021/ie400790v

9 AUTHORS, INCLUDING:

Kevin M Van Geem
Ghent University
101 PUBLICATIONS **859** CITATIONS
SEE PROFILE

Juha Linnekoski
VTT Technical Research Centre of Finland
29 PUBLICATIONS **416** CITATIONS
SEE PROFILE

Antero Laitinen
VTT Technical Research Centre of Finland
19 PUBLICATIONS **118** CITATIONS
SEE PROFILE

Ali Harlin
VTT Technical Research Centre of Finland
113 PUBLICATIONS **898** CITATIONS
SEE PROFILE

I&EC research
Industrial & Engineering Chemistry Research

Article

pubs.acs.org/IECR

Value Added Hydrocarbons from Distilled Tall Oil via Hydrotreating over a Commercial NiMo Catalyst

Jinto M. Anthonykutty,[†,*] Kevin M. Van Geem,[‡] Ruben De Bruycker,[‡] Juha Linnekoski,[†] Antero Laitinen,[†] Jari Räsänen,[§] Ali Harlin,[†] and Juha Lehtonen[⊥]

[†]Process Chemistry, VTT Technical Research Centre of Finland, Biologinkuja 7, Espoo, FI-02044 VTT, Finland

[‡]Laboratory for Chemical Technology, Ghent University, Ghent, Belgium

[§]Stora Enso Renewable Packaging, Imatra Mills, FI-55800 Imatra, Finland

[⊥]Department of Biotechnology and Chemical Technology, School of Science and Technology, Aalto University, PO Box 16100, FI-00076 Aalto, Finland

Supporting Information

ABSTRACT: The activity of a commercial NiMo hydrotreating catalyst was investigated to convert distilled tall oil (DTO), a byproduct of the pulp and paper industry, into feedstocks for the production of base chemicals with reduced oxygen content. The experiments were conducted in a fixed bed continuous flow reactor covering a wide temperature range (325−450 °C). Hydrotreating of DTO resulted in the formation of a hydrocarbon fraction consisting of up to ∼50 wt % nC_{17}+C_{18} paraffins. Comprehensive 2D GC and GC−MS analysis shows that the resin acids in DTO are converted at temperatures above 400 °C to cycloalkanes and aromatics. However, at these temperatures the yield of nC_{17}+C_{18} hydrocarbons irrespective of space time is drastically reduced because of cracking reactions that produce aromatics. The commercial NiMo catalyst was not deactivated during extended on-stream tests of more than 30 h. Modeling the steam cracking of the highly paraffinic liquid obtained during hydrotreatment of DTO at different process conditions indicates high ethylene yields (>32 wt %).

1. INTRODUCTION

Catalytic upgrading of vegetable oils or low grade bioderived oils by hydrotreating has huge potential as a sustainable method for the production of petroleum refinery compatible feedstocks.[1,2] The hydrotreating of bioderived oils produces a high quality paraffinic liquid, which contains *n*-alkanes as major compounds. In addition to fuel properties, these paraffinic liquids with no residual oxygen can also be used as attractive renewable feedstocks for the production of green olefins, and aromatics such as toluene, xylene, and benzene by catalytic reforming[3] or steam cracking.[4,5] Interestingly, the production of ethylene, a platform chemical for polyethylene (PE) by these green catalytic routes would support the sustainable packaging goals of many industries.[6,7]

One of the main challenges of any biobased process is to find an inexpensive and nonfood chain affecting feedstock. During the past decades hydrotreated vegetable oil (HVO) has been produced in several countries on an industrial scale using existing petroleum refining technology, but employing these refined vegetable oils makes these processes not very lucrative.[2] Hence, alternative feeds are being considered such as tall oil. Tall oil, the main byproduct of the Kraft paper production process, is abundant in several North European countries, cheap, and green. It thus meets all the specified criteria to be considered a potentially sustainable feedstock for the production of base chemicals.[8]

Tall oil is a mixture of fatty acids, resin acids, and unsaponifiables; found in pine, spruce and birch trees and used as a resin in many different industries.[9] The main fatty acids in tall oil are oleic, linoleic, and palmitic acids. Resin acids are a mixture of organic cyclic acids, with abietic acid as the most abundant resin acid in tall oil. Unsaponifiable components in the tall oil include hydrocarbons, higher alcohols, and sterols. The fatty and resin acids combination of tall oil offers a good platform to use it as a chemical source upon upgrading.[9,10] Upgrading processes are mainly based on the removal of oxygenates from the bio-oils by hydrodeoxygenation (HDO), supplemented by decarboxylation and decarbonylation in the presence of hydrogen.[11] Conventional hydrotreating catalysts such as cobalt- or nickel-doped Mo on alumina (Al_2O_3) support in sulfide form are usually employed for HDO.[11,12] Zeolites have also been proposed for upgrading in the absence of hydrogen, but oxygenates are mostly converted to carbonaceous deposits and to a lesser extent to paraffin range hydrocarbons.[10,13] Most of the earlier reports on crude tall oil (CTO) are based on an upgrading by zeolites and mainly discuss the production of aromatics and the methods to reduce coking at high temperatures (>400 °C).[9,10,13] More recently, Mikulec et al. investigated the hydrotreating of CTO with atmospheric gas oil (AGO) and reported that NiMo and NiW hydrotreating catalysts can be used for the production of a biocomponent for diesel fuel.[14] Tall oil fractions have also been studied, and several reports are available in literature describing the behavior of tall oil fractions, especially the fatty acid fraction, under hydrotreating conditions.[8,15,16] Different re-

Received: March 11, 2013
Revised: June 24, 2013
Accepted: July 2, 2013
Published: July 2, 2013

action mechanisms have been proposed for the formation of *n*-alkanes, water, CO_2, CO, and propane from fatty acids.[17−20] The behavior of the resin acid fraction is complex under these conditions and the mechanism for its ring rupture is less understood. Coll et al. considered different reaction mechanisms for the hydrotreatment of resin acids in the presence of commercial sulfided NiMo and CoMo catalysts.[8] They found that both the carboxylic group and the unsaturated carbon−carbon bonds in the ring is subjected to the action of hydrogen. On the other hand the thermal or catalytic cleavage of carboxylic acid groups led to the formation of CO_2. In addition, catalytic cracking reactions occur at higher temperatures (≥400 °C) in the presence of NiMo catalyst and hydrogen, causing the ring to open. Catalytic cracking of resin acid have been studied extensively.[21−23] Dutta et al. investigated rosin (resin acids) hydrotreatment under different conditions with $NiMo/Al_2O_3$, Ni−Y zeolite, and ammonium tetramolybdate.[22] This study revealed that NiMo catalysts are active at higher temperatures (≥400 °C), and under these conditions mainly cycloalkanes and aromatics are produced. Şenol et al.[24] confirmed that in particular for aliphatic oxygenates $NiMo/Al_2O_3$ catalysts have good hydrodeoxygenation capabilities.

Most of the studies with tall oil reported in literature deal either with the direct use of CTO or its fractions.[8−10,13−16] The direct use of CTO is less attractive as it contains residual metal impurities, which may cause catalyst deactivation by active site poisoning.[25] Therefore in this contribution the upgrading (hydrotreating) potential of distilled tall oil (DTO) over a commercial NiMo catalyst is studied, focusing on the production of paraffinic liquids as a renewable feedstock especially for steam crackers. It is particularly important for steam cracking that the feedstocks contain little to no oxygen because this creates operating problems in the separation section.[26] Some oxygenates in the reactor effluent, such as formaldehyde,[27] are reactive and can polymerize resulting in serious fouling downstream. Since the separation train of most steam cracking facilities are not equipped to cope with oxygenates, these molecules can end up in the C_3 and C_2 olefin stream. Metallocene catalysts in polymerization processes, which utilize these olefin streams, are poisoned by oxygen components even when they are only present in the ppm level.[26] The presence of trace amounts of methanol in the C_3 splitter propylene stream has led to off speciation polymer grade propylene.[28] DTO, a product of vacuum distillation of CTO contains mainly fatty acids (∼70%) and a minor amount of resin acids (*ca.* 25−30%). The use of DTO as a direct chemical source for upgrading is less studied and the detailed composition of the upgraded product is not known in literature, although it has been reported that the upgraded DTO can be used as a potential feedstock in conventional steam crackers.[5,29] Furthermore, in view of the literature,[22,24] the HDO and hydrocracking activity of the NiMo catalyst is assessed for DTO over a wide temperature range (325−450 °C), which is not reported elsewhere. The evaluation of product distribution obtained from high temperature experiments is of particular interest in this study as improving the understanding of nature of the ring rupture of resin acids to cycloalkanes and other hydrocarbons (saturated/unsaturated). Additionally, the formation of aromatics especially from resin acids in high temperature reactions is evaluated. In the present research approach, different process conditions based on temperature and space velocity (WHSV) are tested, and the most suitable conditions are applied to perform a stability test run.

2. MATERIALS AND METHODS

2.1. Materials. Commercially available DTO, obtained from pulping of Norwegian spruce was used as received. The detailed acid composition and elemental composition of the employed SYLVATAL 25/30S, DTO is as shown in Table 1. Commercial

Table 1. Elemental and Detailed Acid Composition of Distilled Tall Oil (DTO)

	DTO
Elemental Composition [%] D 5291	
carbon	77.4
hydrogen	11.1
nitrogen	<0.1
sulfur	0.05
oxygen	11.5
detailed acid composition [wt %] GC−MS	
free fatty acids (FFA)	71.3
(16:0) palmitic acid	0.2
(17:0) margaric acid	0.3
(18:0) stearic acid	0.7
(18:1) oleic acid	15.3
(18:1) 11-octadecenoic acid	0.5
(18:2) 5,9-octadecadienoic acid	0.3
(18:2) conj. octadecadienoic acid	8.3
(18:2) Linoleic acid	24.3
(18:3) Pinolenic acid	4.4
(18:3) Linolenic acid	0.6
(18:3) conj. octadecatrienoic acid	1.8
(20:0) arachidic acid	0.4
(20:3) 5,11,14-eicosatrienoic acid	7.6
(22:0) behenic acid	0.6
other fatty acids	6.0
resin acids	23.0
8,15-isopimaradien-18-oic acid	0.5
pimaric acid	4.8
sandaracopimaric acid	0.3
diabietic acid	0.5
palustric acid	2.2
isopimaric acid	1.1
13-*B*-7,9(11)-abietic acid	0.4
8,12-abietic acid	0.3
abietic acid	7.7
dehydroabietic acid	3.6
neoabietic acid	0.4
other resin acids	1.3

NiMo (1.3 Q) catalyst was purchased and used in sulfided form. GC grade standards *n*-octadecane (Restek, Florida, 99%), *n*-octatriacontane (Restek, Florida, 99%), Restek, Florida, TRPH standard (C_8−C_{38}), *trans*-decahydronaphtalene (Aldrich, 99%), 1,2,3,4-tetrahydronaphtalene (Fluka, 99.5%), and 5-α-androstane solution (Supelco) were purchased and used for GC−MS calibration. The gases used in the experiment were obtained from AGA. The purity of gases was ≥98.2% for H_2S and 99.99% for H_2.

2.2. Experimental Conditions. Catalytic upgrading (HDO) of DTO was conducted in a continuous, down flow, fixed bed reactor. The reactor was 450 mm long, 15 mm internal diameter stainless steel tube, fixed coaxially in a furnace, as shown in Figure 1.

The studied amounts of fresh catalyst were 2, 3, and 6 g. The catalyst bed was fixed with quartz wool (approximately 0.8g) on

dx.doi.org/10.1021/ie400790v | *Ind. Eng. Chem. Res.* 2013, 52, 10114−10125

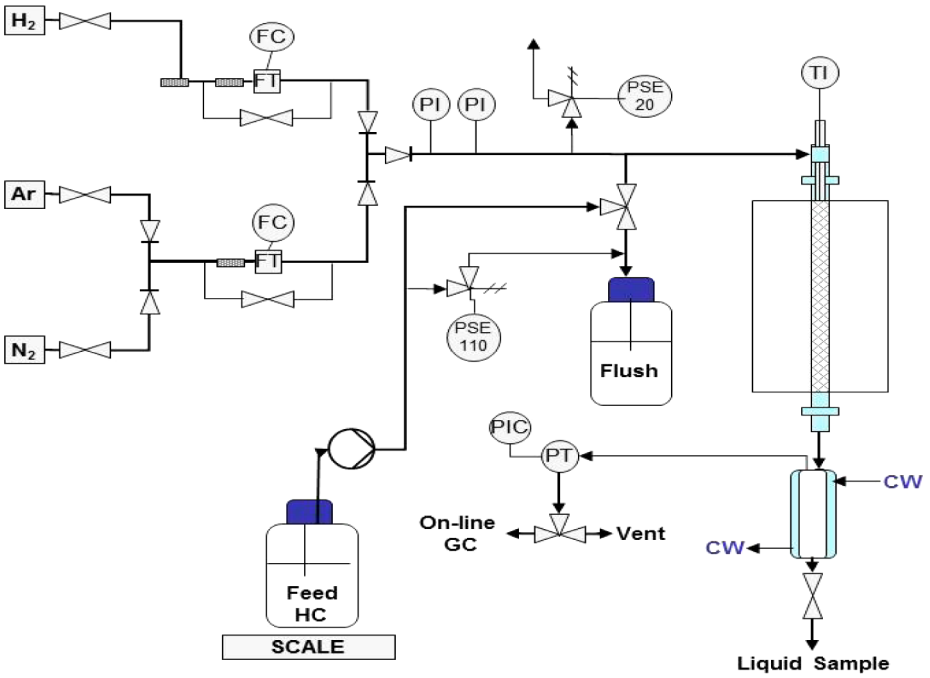

Figure 1. Schematic representation of fixed bed reactor setup.

a supporting pin in the middle of the reactor tube. A thermocouple for temperature measurements was placed in the middle of the catalyst bed (accuracy ±0.1 °C). A pressure test was carried out at 4−5 MPa (Ar, >99%) for 2−3 h. Prior to catalyst activation the catalyst was dried. Drying started at room temperature under nitrogen flow (>99%, 2.2 L/h) and continued until the reactor reached 400 °C in 2 h under atmospheric pressure. After reaching 400 °C, the reactor was kept isothermal under nitrogen flow for 30 min, prior to presulfidation. The presulfidation was carried out by using a H_2S/H_2 mixture for 5 h at 400 °C (H_2S/H_2 = 5 vol %). Following presulfidation, the temperature was set to the reaction temperature and the reactor was pressurized to 5 MPa with hydrogen (99.99%). The experiments were conducted in a temperature range of 325−450 °C under 5 MPa hydrogen pressure. The feed line was heated to 120 °C prior to an experiment and the liquid feed was fed into the reactor with a fixed feed rate of 6 g/h ± 0.1 g/h in all experiments. The catalyst bed volume was varied in order to study the effect of varying weight hourly space velocities (WHSV = 1, 2, and 3 h^{-1}). In all experiments a molar ratio 17.4 of H_2 to DTO (62 mol/kg DTO) was used, which is higher than the required amount (25 mol/kg feed) for complete deoxygenation of pyrolysis oils obtained from forest residues.[30,31] With DTO, a rough theoretical calculation of stoichiometric amount (in moles) of H_2 needed to make complete hydrogenation and deoxygenation was carried out, and the calculated amount is ∼20 mol/kg of DTO. The higher molar ratio (H_2 to DTO) used in this approach can be justified with the fact that excess hydrogen flow is needed to remove the water formed during hydrodeoxygenation and thereby prevent the catalyst from deactivation.[32] During an experiment, after the stabilization period (6 h) a liquid sample was collected and fractionated into an organic and aqueous phase.

2.3. Analytical Methods. The detailed analysis of organic phase was carried out by GC−MS. An Agilent GC−MS instrument equipped with a HP-5 MS column (30 m × 0.25 mm × 0.25 μm) was used for analysis. Samples were diluted with either hexane or dichloromethane prior to the analysis. The weight fractions were calculated using an external calibration method. The major products such as *n*-alkanes and *i*-alkanes were quantitatively analyzed using the response factors of *n*-octadecane, *n*-octatriacontane, and Restek, Florida, TRPH standard (C_8−C_{38}). Moreover, aromatics and other nonaromatic products (cyclics) were analyzed using the response factors of 1,2,3,4-tetrahydronaphthalene and 5-α-androstane (same as the response of *n*-octadecane), respectively. The detailed composition of organic phase was also determined using GC × GC-FID/(ToF-MS) equipped with a typical polar (Rtx-1 PONA, 50 m × 0.25 mm × 0.5 μm)/medium-polar (BPX-50, 2 m × 0.15 mm × 0.15 μm) column combination and cryogenic liquid CO_2 modulator. The modulation period was 5 s. The oven temperature was gradually increased from 40 to 300 °C at 3 °C/min. The samples were diluted with *n*-hexane and injected with a split ratio of 1:250. The enhanced resolution obtained with this technique proved to be crucial to accurately quantify the small amounts of polycyclic components in the hydrotreated DTO. The quantitative and qualitative information obtained from GC−MS and GC × GC-FID/TOF-MS was combined. The accuracy of the GC−MS analysis was ±15% for quantitatively analyzed products, that is, the products analyzed based on the response factor obtained from exact external standards (octadecane and 1,2,3,4-tertahydronaphthalene) and ±30% for all other semiquantitatively (quantification based on the response factor obtained from a model external standard for the analyte) analyzed products. The settings of the GC−MS and GC × GC can be found in the Supporting Information.

The elemental composition of DTO and the organic phase was analyzed using CHN equipment (Variomax) based on the standard ASTM D 5291 method. Sulfur content in samples was determined by the ASTM D 4239 method. The elemental composition of oxygen in the sample was calculated by subtracting the sum of CHN-S composition from 100,

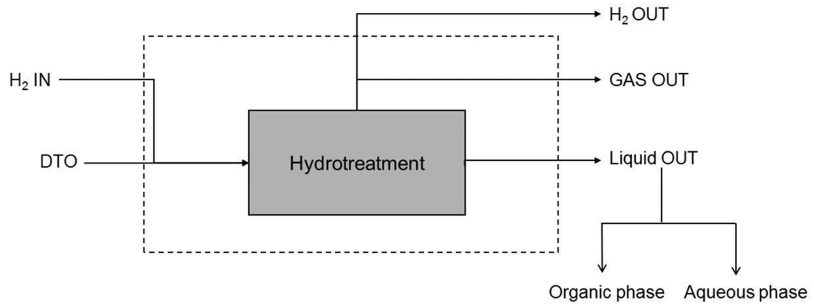

Figure 2. Procedure to calculate the overall mass balance.

assuming that the sample contains no other elements than C, H, N, S, and O. The acid composition of DTO and the organic phase was analyzed using a gas chromatograph equipped with DB-23 column (25−30 m × 0.25 mm × 0.20 μm) and a flame ionization detector (method: ASTM D 5974-00, TMPAH methylating agent, and myristic acid as an internal standard). Water content in the aqueous phase was measured by using Karl Fischer (KF) titration (method: ASTM E 203). Gas phase components were analyzed using a FT-IR instrument (Gasmet). The latter was calibrated for each component in the gas phase in a range that corresponds to the range expected in the product stream. Total acid number (TAN) of products and feed was calculated by ASTM D 664 method.

2.4. Calculations. The conversion (X) of acids was calculated by the following equation by assuming that residual acids are predominantly present in the organic phase.

$$X\ (\%) = \frac{n_{\mathrm{A,feed}} - n_{\mathrm{A,OP}}}{n_{\mathrm{A,feed}}} 100$$

where $n_{\mathrm{A,feed}}$ is the total mole of acids (fatty acid/resin acid) present in the feed, $n_{\mathrm{A,OP}}$ is the total mole of acids (fatty acid/resin acid) present in the organic phase, obtained by GC analysis.

The degree of deoxygenation (DOD) was calculated as follows:

$$\mathrm{DOD}\ (\%) = \left[1 - \frac{\text{mass of oxygen in OP}}{\text{mass of oxygen in feed}}\right] 100$$

The total mass balance estimation was carried out based on the scheme shown in Figure 2. Liquid products were separated into organic and aqueous phases, and the amount of water (wt %) from the aqueous phase was measured. At lower temperatures the total mass balance could be closed within 3% on average. The increase in mass balance error (max 6%) with increase of temperature is attributed to the increase in formation of gaseous and other cracking products at higher temperatures which were not measured.

3. EXPERIMENTAL RESULTS

3.1. Effect of Process Conditions on Product Distribution. The effect of reaction temperature and space time on overall distribution of product fractions obtained during hydrotreating of DTO is given in Table 2. The weight fraction of the fractionated organic phase decreases for all studied WHSVs as a function of temperature. The aqueous phase mainly contained water and also a small concentration (~5−10 wt % of aqueous phase) of partly solid fine white particles. These partly solid particles are very probably intermediary products from catalytic reactions (fatty acids, alcohols, fatty acid esters, etc.) as observed also by Mikulec et al.[18] For the remainder of the study these components are considered as unaccounted products. The cloudiness of the aqueous phase due to the presence of unaccounted products increased with shorter space times (WHSV = 2 and 3 h^{-1}), especially at lower temperatures (<375 °C) and often resulted in additional difficulties for the separation of the organic phase from the aqueous phase. As expected the amount of formed gas increased with temperature, which is obviously related to the increased cracking reactions that occur at higher temperatures.[19,33]

Major products obtained from detailed GC−MS and GC × GC-FID/TOF-MS analysis of the organic phase are reported in Figure 3. Individual products identified in the organic phase include *n*-alkanes, *i*-alkanes, cyclics, and aromatics, and are discussed separately in Table 3. The GC × GC chromatogram obtained for the major components of HDO−DTO is as shown in Figure 4.

Paraffins. *n*-Alkanes and *i*-alkanes obtained during the process are collectively denoted as paraffins in this section. *n*-Octadecane (*n*-$C_{18}H_{38}$), which was found to be the major *n*-alkane, is obtained as a result of hydrodeoxygenation (HDO) reaction from C_{18} fatty acids. *n*-Heptadecane (*n*-$C_{17}H_{36}$), obtained from hydrodecarbonylation and hydrodecarboxylation of the same compounds (C_{18} acids)[15−20,34] was also found as a major *n*-alkane. As shown in Table 3, the concentration of *n*-octadecane and *n*-heptadecane was higher at low temperatures (<400 °C). It is also apparent that space time has an influence on the production rate of *n*-C_{18} and *n*-C_{17} as their concentration increased with an increase in space time. At low temperatures (≤400 °C), *n*-C_{18} + C_{17} were obtained in a range of 19−50 wt % throughout all experiments. The minimum yield (19 wt %) was obtained at the lowest reaction temperature (325 °C), and the shortest space time (WHSV = 3 h^{-1}) or at the highest temperature (450 °C) and the longest space time (1 h^{-1}) (15.1 wt %). As can be seen from Table 3, isomerization of *n*-alkanes occurred at all reaction conditions and increased almost linearly with temperature.

Cyclics. As illustrated by Figure 3, monocyclic and polycyclic compounds obtained from fatty and resin acids were obtained in a range of 6.1−24.3 wt % in all experiments. 18-Norabietane (MW, 262) is identified as a major cyclic primary product in low temperature experiments (<375 °C), which is presumably formed from abietic-type resin acids by the hydrodeoxygenation reaction.[8] Other resin acids (pimaric acid, palustric acid, and isopimaric acid) present in DTO may also undergo primary reactions and produce corresponding cyclic hydrocarbons (MW, 274; and MW, 260). As shown in Table 3, the concentrations of primary cyclic products (mainly 18-norabietane) from resin acids decrease with temperature. As

Table 2. Overall Product Distribution Obtained from Hydrotreating Experiments of DTO on a Commercial NiMo Catalyst

temp (°C)	325	350	375	400	425	450	325	350	375	400	425	450	325	350	375	400	425	450
WHSV (h^{-1})	1	1	1	1	1	1	2	2	2	2	2	2	3	3	3	3	3	3
product distribution (wt %)[a]																		
liquid product																		
organic phase	85.0	83.2	84.0	77.0	77.6	72.0	85.0	78.2	79.5	78.7	76.2	73.0	84.2	80.6	79.2	78	77.3	74.7
water	11.3	10.7	11.5	12.3	10.4	9.9	10.2	11.3	12.9	12.0	10.1	9.5	5.6	7.9	11.5	11.1	11.8	11
unaccounted	0.2	0.3	0.4	0.1	0.2	0.2	2.3	4.6	0.7	4.9	0.8	0.1	6.1	5.8	1.3	0.7	0.2	0.2
total	**96.6**	**94.2**	**95.9**	**89.4**	**88.3**	**82.2**	**97.5**	**94.1**	**93.2**	**95.7**	**87.1**	**82.7**	**96.0**	**94.4**	**92.1**	**89.9**	**89.4**	**86**
Gas product (wt %)	6.0	7.1	8.2	10.3	11.9	14.8	4.5	5.4	7.6	9.9	11.8	13.9	4.0	5.3	7.4	9.4	11.3	12.6
mass balance[b]	−2.6	−1.2	−4.1	0.2	−0.2	2.9	−2	0.3	−0.8	−5.6	1.1	3.3	−0.1	0.2	0.4	0.6	−0.7	1.3

[a]Product distribution (wt %) calculated based on the amount of DTO fed into the reactor. [b]Mass balance estimated excluding H_2 IN and H_2 OUT.

the temperature increases, the hydrocracking behavior (cracking off side chain and ring-opening) of these primary products increases, which results in the formation of mono-, di- and tricycloalkanes. GC−MS analysis also shows the presence of monocyclic C_{17}−C_{18} hydrocarbons in products from low temperature reactions (<375 °C) irrespective of space time. These monocyclic hydrocarbons are presumably formed from *n*-alkanes and their concentrations decrease with increase of temperature at the expense of more monocyclics of C_7−C_{12} range in high temperature reactions.

Aromatics. Alkyl aromatics (substituted benzenes) and norabietatrienes (MW, 256−258) were the major aromatics identified. 18-Norabieta-8,11,13-triene was obtained as a main primary product probably from abietic acid by decarboxylation/dehydrogenation reaction at low temperatures (<375 °C).[22,23] Table 3 shows that the concentration of norabietatrienes decreases with temperature. A partially deoxygenated product (MW, 258), probably an aromatic ketone intermediate was also observed in low temperature reactions. The concentration of other aromatics such as anthracenes, phenanthrenes, naphthalenes, indenes, 1,2,3,4 tertahydronaphthalene, and alkyl benzenes were found to increase with temperature. This trend is more prominently visible in the experiments with longer space times.

Other Products. Not only the main products, but noticeable amounts of olefins, fatty acid methyl esters, fatty alcohols, and aromatic alcohols were identified especially at lower temperatures by GC−MS and GC × GC-FID/TOF-MS, shown in Figure 3 and Table 3 as other hydrocarbons. Residual acids were not detected completely by these analytical methods and denoted as unidentified in Table 3. These unidentified compounds also include undetected nonaromatic and aromatic hydrocarbons other than residual acids. The detailed analysis of the gas fractions revealed that the major components present in the gas fraction are CO, CO_2, methane, propane, and ethane. CO and CO_2 are produced by hydrodecarbonylation and hydrodecarboxylation/decarboxylation reactions, respectively, and their concentrations are higher at lower temperatures (325−400 °C). The concentration of CO_2 was found to be still significant beyond 400 °C, indicating the possible thermal cleavage of carboxylic group at this stage. Propane and ethane were produced as a result of cracking reactions at high temperatures. Apparently, methane resulted from the methanation reaction of CO and H_2. In addition to these reactions the water gas shift reaction may also be responsible for part of the produced CO_2 and H_2.[15,16]

3.2. Residual Acid Composition and Degree of Deoxygenation. Figure 5 summarizes the residual acid compositions in the organic phase and also the conversion of acids at different space velocities as a function of temperature. Acid compositions with space velocities 1, 2, and 3 h^{-1} are shown in Figure 5 panels a, b, and c, respectively.

At the lowest temperature (325 °C) fatty and resin acid conversions are significantly higher with longer space times (WHSV = 1 h^{-1}). Conversion increased linearly with temperature and reached a maximum value at 375−400 °C for both acids irrespective of space time. Beyond 400 °C, a decrease in conversion of acids was observed with all space times. Maximum acid conversions (98% and 100%, respectively, for fatty and resin acids) were obtained with longer space time. It is noteworthy that the decrease in the conversion of fatty acid at higher temperatures (>400 °C) with longer space time (WHSV = 1 h^{-1}) was slightly more pronounced than the

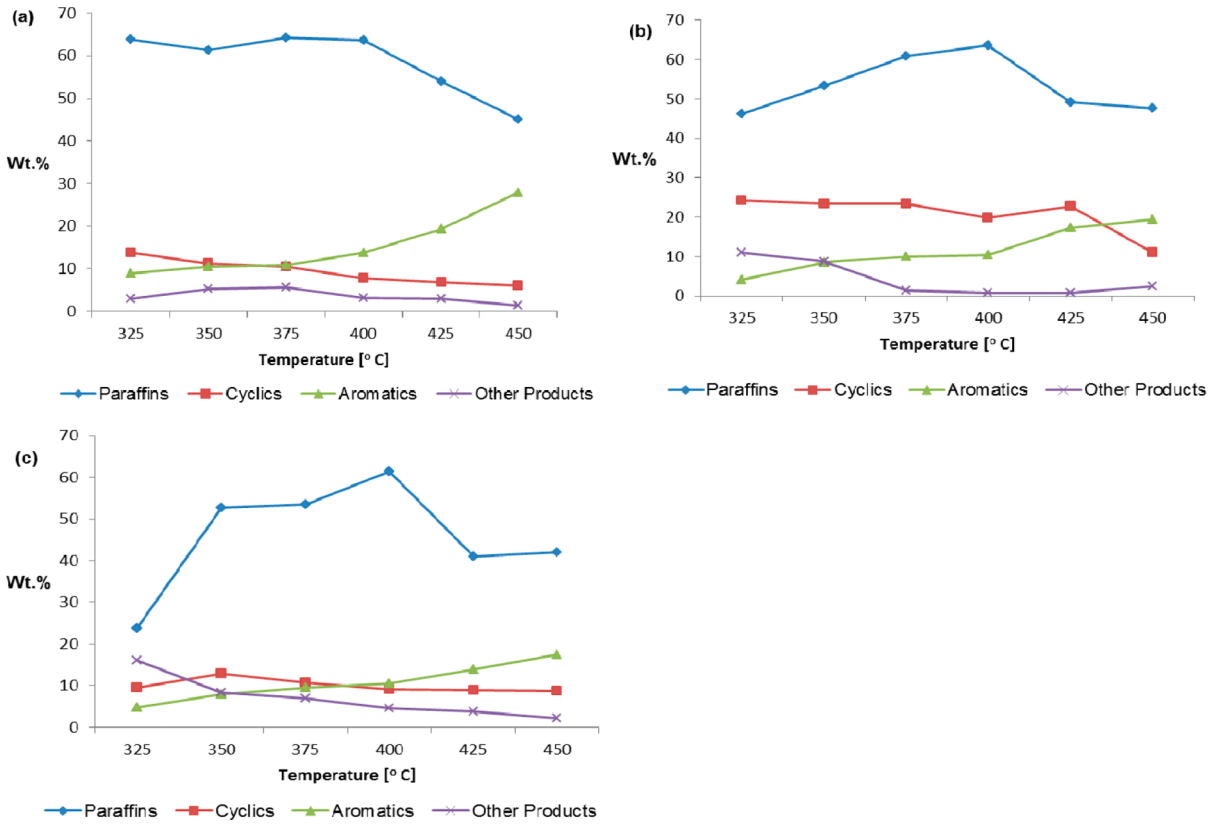

Figure 3. Major products obtained during the hydrotreating of DTO at different process conditions: (a) WHSV= 1 h^{-} (b) WHSV= 2 h^{-1} (C) WHSV= 3 h^{-1}.

decrease in conversion with shorter space times (WHSV = 2 and 3 h^{-1}). Total acid number (TAN) analyses of products showed that the minimum value (0.1 mgKOH/g) of TAN corresponding to DTO feed (0.3 mgKOH/g) was also obtained during experimental runs conducted at longer space time.

The degree of deoxygenation was calculated for all experiments and is presented in Figure 6. These results clearly show that the deoxygenation rate was higher in low temperature (325−375 °C) runs with longer space time (WHSV 1 h^{-1}). At low temperatures selective deoxygenation is a favorable reaction, that is, oxygen is eliminated in the form of water, CO_2, and CO, and it occurs by several reaction routes such as hydrodeoxygenation, hydrodecarboxylation, and hydrodecarbonylation reactions. Additionally, deoxygenation via decarboxylation is supposed to take place without any requirement of hydrogen and presumably proceeds only by cleavage of carboxylic group as proposed by several researchers,[8,34−37] in particular by Kubička et al., as they propose different dexoygenation pathways for pure sulfided Ni and Mo catalyst as well as NiMo catalyst based on the electronic properties of Ni and Mo.[34] Different competing reaction routes occur during the deoxygenation process, and their favorable conditions can be understood in detail from the reaction scheme proposed for the hydrotreating of DTO, in view of literature,[33,34,36,8,22,23] represented as Scheme 1.

As the temperature increases (>375 °C), selective deoxygenation reactions are less favored and at this stage presumably dexoygenation mainly occurs by nonselective deoxgenation, that is, by cracking, which produces intermediate oxygenates, hydrocarbons, and CO_2.[37] The maximum deoxygenation rate achieved in low temperature runs with longer space time explains that selective deoxygenation is the major deoxygenation route, which enables the complete deoxygenation during hydrotreating process. However, it can also be assumed that the synergistic effect of selective and nonselective deoxygenation might also play a role for increasing the deoxygenation rate at feasible reaction temperature (375−400 °C) for both routes.

3.3. Catalyst Stability. Figure 7 shows the results obtained from a 32 h stability test run performed with DTO over the NiMo catalyst at 350 °C, 5 MPa, 2 h^{-1} WHSV, and with a H_2 to DTO molar ratio of 17. The samples were collected at different time intervals and the organic phase was analyzed using GC × GC-FID/TOF-MS. As noted from Figure 7, the product composition did not change too much within the experimental error, that is, a sign of deactivation, was not observed during the 32 h stability test and it can be perceived that the catalyst exhibited a stable activity as a function of time-on-stream (TOS). The concentration of main product, nC_{17}+C_{18} varied between 41 and 48 wt %. Other monitored products were aromatics, cyclics, *i*-alkanes, esters, and olefins. Even though the test run duration was not long enough to assess the stability in industrial operation for several months, the results presented in this work give an indication that DTO can be hydroprocessed over a commercial NiMo catalyst for a considerable period of time without any noticeable catalyst deactivation.

4. DISCUSSION

4.1. Reaction Mechanism Assessment. The overall product distribution obtained from the upgrading studies of DTO at different process conditions is in line with earlier studies with HVO.[19,33] In this case, variation in space time has

dx.doi.org/10.1021/ie400790v | *Ind. Eng. Chem. Res.* 2013, 52, 10114−10125

Table 3. Product Distribution of the Organic Phase from Hydrotreating Experiments of DTO

temp (°C)	325	350	375	400	425	450	325	350	375	400	425	450	325	350	375	400	425	450
WHSV (h^{-1})	1	1	1	1	1	1	2	2	2	2	2	2	3	3	3	3	3	3
composition (wt %)																		
s hydrocarbons																		
nC_7–C_9	0.2	0.5	0.8	1.4	3.3	5.5	0.3	0.5	1.1	2.9	3.3	3.8	0	0.2	0.5	1.2	2.6	4.3
nC_{10}-C_{16}	0.8	1.6	2.7	4.5	8	10.2	0.9	1.4	2.1	2.2	9	9.6	0.1	0.8	1.7	3.9	6.6	8.4
nC_{17}	13.1	12.6	16.7	19.7	12.4	5.1	8.4	13.8	17.3	17.2	13.9	10.8	5.2	12.3	15.9	18.7	9.8	5.3
nC_{18}	36.6	33.6	27.5	21.9	15.9	10	27.1	27	26.8	26.4	13.6	10.2	13.8	27.5	22.7	21.6	12.4	14.3
nC_{19}	3.1	2.8	3.5	4	2.6	1.1	1.6	2.3	3.1	3	2.2	2.2	1.2	2.8	3.4	4.1	2.7	1.3
nC_{20}	6.3	5.1	3.9	3	2	1.1	3.6	3.8	3.7	3	1.6	1.4	2.1	4.2	3.4	3.2	1.8	2
nC_{20+}	0.8	1.5	3	1.1	0.6	0.1	2.6	1.6	2.2	2.2	1.6	0.5	0.4	1.6	2	2.7	1	0.4
*i*alkanes	3	3.7	6.1	8.1	9.1	12	1.4	2.5	4.2	6.3	7.2	9.2	1	3.2	3.9	5.9	4.1	6
total	**63.9**	**61.4**	**64.2**	**63.7**	**53.9**	**45.1**	**46.3**	**53.3**	**60.8**	**63.5**	**49.2**	**47.7**	**23.8**	**52.6**	**53.5**	**61.4**	**41**	**42**
Non-aromatics																		
18-norabietane	10.4	7.2	1.6	0.3	0	0	13.7	15.3	11.1	5.6	5.9	0	4.4	9.4	2.9	1.3	0.3	0
cycloalkanes	3.3	4.1	8.7	7.4	6.6	6	10.6	8.1	12.2	14.2	16.9	11	5.1	3.4	7.7	7.9	8.6	8.7
o HC	2.9	5.2	5.7	3.2	2.9	1.4	11	8.7	1.4	0.8	0.7	2.4	16	8.3	7	4.6	3.8	2.1
total	**16.6**	**16.5**	**16.1**	**10.9**	**9.6**	**7.5**	**35.3**	**32.1**	**24.7**	**20.6**	**23.5**	**13.4**	**25.5**	**21.1**	**17.6**	**13.8**	**12.7**	**10.8**
aromatics																		
norabietatrienes	3.4	2.2	0.9	0	0	0	3.7	6.3	4.3	3.3	2.7	0	1.4	5.3	2.4	1.1	0.1	0
other aromatics	5.6	8.2	9.8	13.8	19.4	27.8	0.5	2.2	5.7	7.1	14.6	19.3	3.2	2.7	7	9.3	13.8	17.5
Total	**9**	**10.4**	**10.8**	**13.8**	**19.4**	**27.8**	**4.2**	**8.5**	**10**	**10.4**	**17.3**	**19.3**	**4.7**	**8**	**9.4**	**10.5**	**13.9**	**17.5**
overall wt %	**89.6**	**88.4**	**91.1**	**88.4**	**83**	**80.4**	**85.8**	**93.9**	**95.6**	**94.5**	**90**	**80.4**	**54.1**	**81.7**	**80.7**	**85.7**	**67.7**	**70.4**
unidentified	10.3	11.5	8.8	11.6	17	19.5	14.1	6	4.3	5.5	9.9	19.6	45.8	18.2	19.2	14.2	32.2	29.5

dx.doi.org/10.1021/ie400790v | *Ind. Eng. Chem. Res.* 2013, 52, 10114−10125

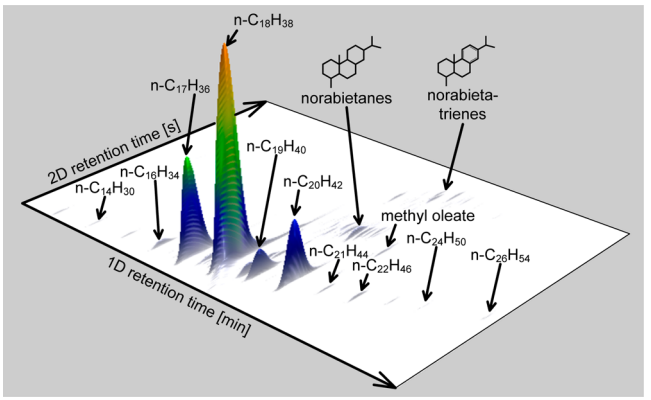

Figure 4. GC × GC-FID chromatogram (3D representation) of HDO–DTO indicating the most important components:[5] WHSV = 2 h^{-1}, T = 350 °C, P = 5 MPa.

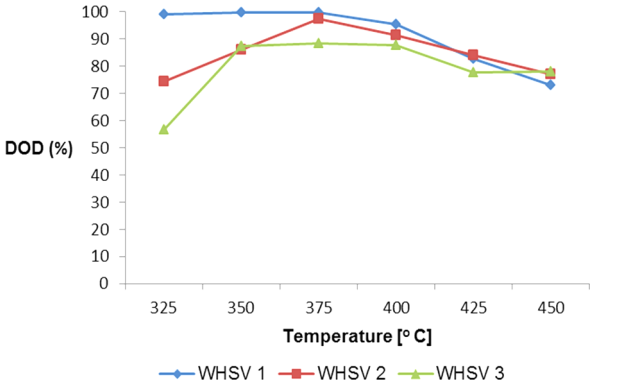

Figure 6. Influence of the temperature and space time on degree of deoxygenation (DOD): WHSV= 1–3 h^{-1}, T = 325–350 °C, P = 5 MPa.

also a less pronounced effect than temperature on the product yields as can be seen in Table 2. Several different reaction routes represented in Scheme 1 explain the wide distribution of products. The formation of *n*-heptadecane and norabietatrienes by a noncatalytic route is confirmed as they appeared in the product stream of runs conducted at 350 and 450 °C in the absence of catalyst. The reaction mechanism from fatty acids has been explained in detail in several studies.[15,16,35,36] These studies propose that different deoxygenation mechanisms prevail at low and high temperatures, and the requirement of hydrogen for these deoxygenation routes would be different. At low temperatures (<375 °C), hydrodeoxygenation is the most favorable reaction occuring with maximum requirement of hydrogen compared to hydrodecarboxylation and hydrodecarbonylation.[35,36] This fact is evident on the basis of the higher yield of *n*-octadecane obtained in this study in low temperature runs. The significant role of the hydrodecarboxylation route at higher temperatures is validated with the higher yield of *n*-heptadecane obtained at temperatures (400 °C) above optimum reaction temperature range (325–375 °C). Furthermore, the C–C splitting of the fatty acid chain may occur prior to cleavage of the carboxylic acid function (nonselective deoxygenation) at higher temperatures, and apparently results in the formation of shorter fatty acid chains

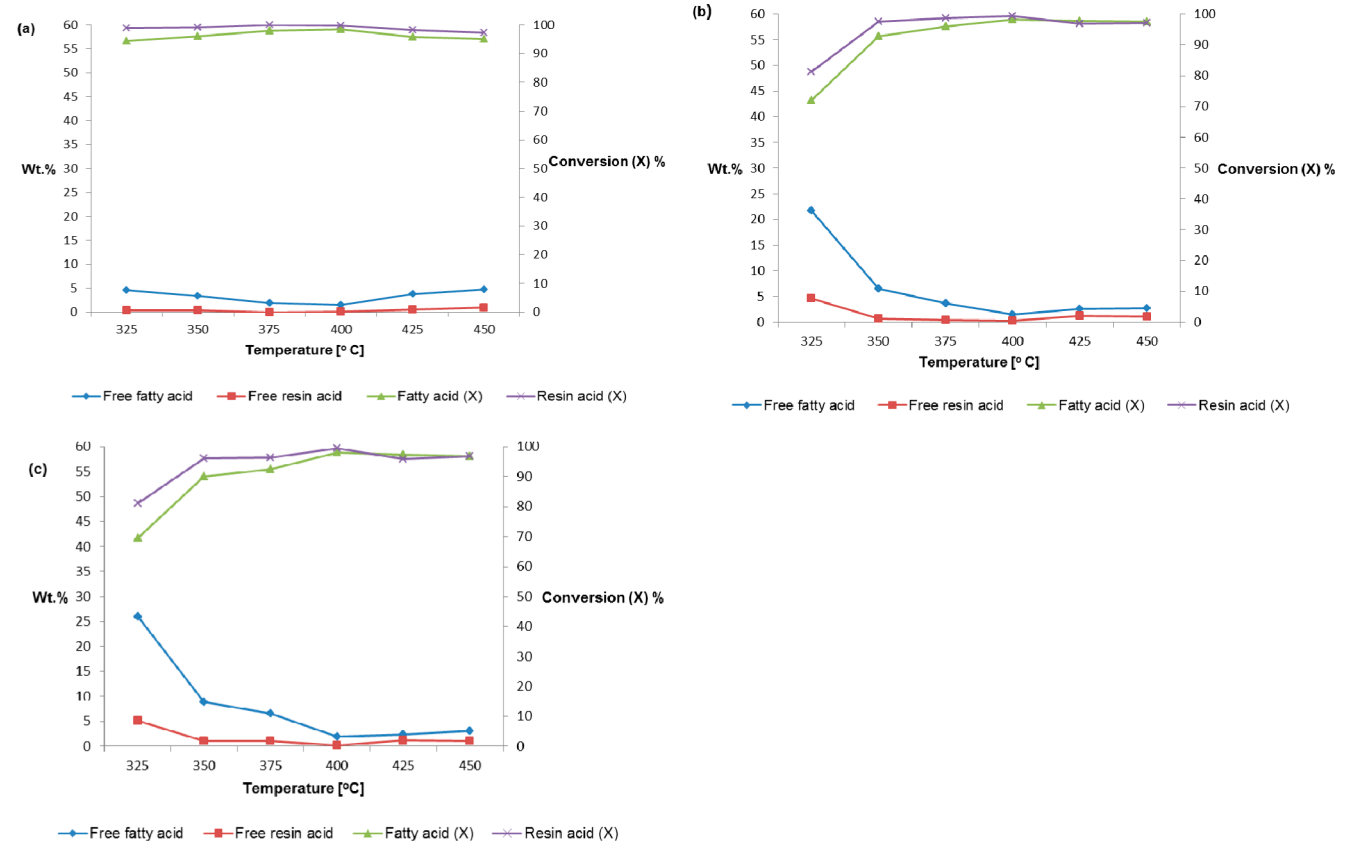

Figure 5. Residual compositions and conversions of acids at different space times T = 325–350 °C: (a) WHSV= 1 h^{-1} (b) WHSV= 2 h^{-1} (c) WHSV= 3 h^{-1}.

dx.doi.org/10.1021/ie400790v | *Ind. Eng. Chem. Res.* 2013, 52, 10114–10125

Scheme 1. Simplified Reaction Network Proposed for the Hydrotreating of DTO

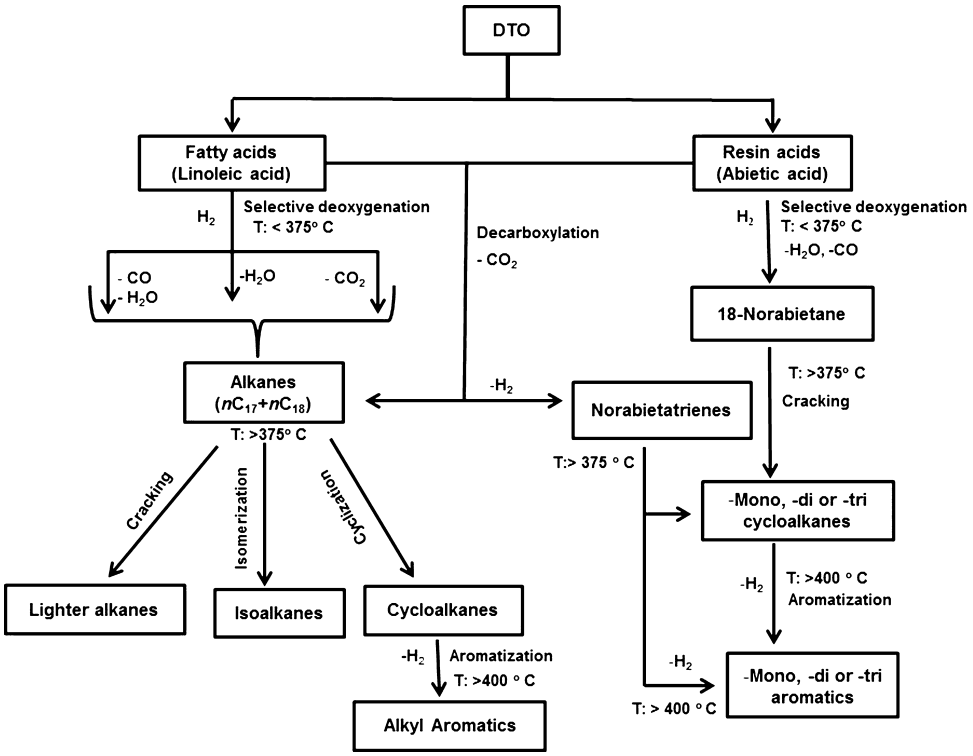

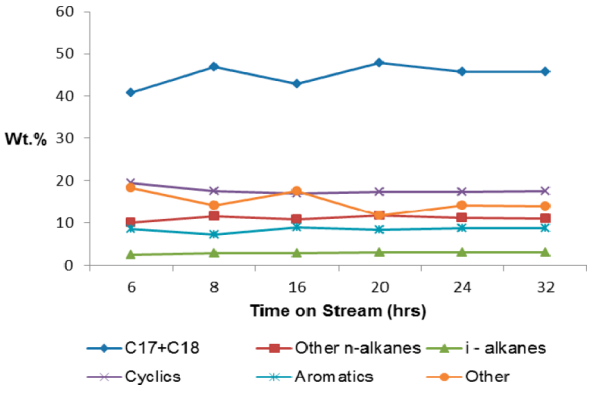

Figure 7. Product distribution as function of time-on-stream during a 32 h stability test: WHSV= 2 h^{-1}, T = 350 °C, P = 5 MPa.

especially with longer space times. These shorter fatty acids are less reactive at higher temperatures as proposed by Kubičková et al.[37] These findings in literature also support the results shown in Figure 5a–c; that is, decrease in conversion of fatty acids with increase of temperature especially with longer space times.

With resin acids, the reaction mechanism is more complex and it can be assumed that catalytic deoxygenation occurs via a hydrogenation/dehydrogenation pathway to form primary tricyclic structures.[22,38] The occurrence of parallel hydrogenation and dehydrogenation routes is evident in this approach as significant yields of both abietane-type structures and norabietatrienes were obtained in low temperature runs (<400 °C). The disappearance of 18-norabieta-8,11,13-triene with increase of temperature clarifies that norabietatrienes are further dehydrogenated to form mono-, di- or triaromatics with the severity of reaction temperature, as proposed by Dutta et al.[22] It is also noteworthy that primary tricyclic structures (18-norabietane) presumably formed by complete hydrogenation and deoxygenation are consumed in high temperature reactions and produce more aromatics through intermediate cycloalkanes. However, the fully aromatic retene-type structures were not detected by GC–MS analysis, which signifies the nonoccurrence of complete dehydrogenation in this study. Unlike fatty acids, the C–C splitting from certain resin acids (diabietic acid and dehydroabietic acid), is apparently minimal at high temperatures before the carboxylic group is removed.[23] These resin acids may partly remain intact during this stage as the removal of the carboxylic function might not be complete by less favorable selective deoxygenation reactions occurring at higher temperatures.

However, it should be noted that in comparison with studies of rapeseed oil, palm oil, and sunflower oil[18] under similar conditions (NiMo/γ- Al_2O_3 catalyst, T = 350 °C and P = 4.5 MPa, LHSV: 0.6–0.8 h^{-1}), the employed DTO gives a lower amount of $nC_{17}+C_{18}$ at low temperatures (≤400 °C) irrespective of the space time. It is clearly in accordance with earlier studies of Monnier et al.[36] and Kikhtyanin et al.[19] that the composition of fatty acids has a significant influence on the distribution of n-alkanes. However, at high temperatures (>400 °C), the amount (16–29 wt %) of $nC_{17}+C_{18}$ with DTO was found to be much higher than the yield (4.6 wt %) obtained with sunflower oil (pH_2 =18 MPa, T = 420 °C, and WHSV = 0.7 h^{-1}) over a similar commercial hydrotreating catalyst.[39]

4.2. Application of Deoxygenated DTO as a Renewable Feedstock for Steam Crackers. Optimization of the process conditions of the NiMo catalyst resulted in a high degree of deoxygenation. The distribution of n-alkanes with a maximum yield of 50 wt % $nC_{17}+C_{18}$ obtained from DTO at low temperatures (<400 °C) clearly shows the potential of these fractions to be used as a feedstock in steam crackers for the production of green olefins.[5] Therefore the detailed product yields have been determined using COILSIM1D[29] under

dx.doi.org/10.1021/ie400790v | Ind. Eng. Chem. Res. 2013, 52, 10114–10125

Table 4. Product Distribution for Steam Cracking of the Organic Phase As Function of WHSV and Hydrotreating Temperature[a]

HDT temp (°C)	325	350	375	400	425	450	325	350	375	400	425	450	325	350	375	400	425	450	325	350	375	400	425	450
HDT WHSV (h^{-1})	1	1	1	1	1	1	2	2	2	2	2	2	3	3	3	3	3	3						
composition of cracker effluent (wt %)																								
hydrogen	0.5	0.5	0.5	0.5	0.5	0.6	0.5	0.5	0.5	0.5	0.5	0.5	0.5	0.5	0.5	0.5	0.5	0.5	0.5	0.5	0.5	0.5	0.5	0.5
methane	9.6	9.5	9.5	9.6	9.6	9.6	9.3	9.4	9.6	9.8	9.5	9.5	8.6	9.4	9.3	9.5	9.3	9.5	9.3	9.4	9.3	9.5	9.3	9.5
carbon monoxide	0.4	0.5	0.3	0.4	0.6	0.6	0.6	0.2	0.2	0.2	0.3	0.7	1.9	0.7	0.8	0.5	1.1	1.0	1.9	0.7	0.8	0.5	1.1	1.0
carbon dioxide	0.7	0.7	0.5	0.7	0.9	0.9	0.9	0.4	0.3	0.3	0.5	1.0	2.9	1.1	1.2	0.8	1.8	1.5	2.9	1.1	1.2	0.8	1.8	1.5
ethene	32.2	32.1	32.1	32.3	32.2	31.8	31.0	30.8	31.5	32.3	31.5	32.0	31.7	31.7	32.1	32.5	32.6	32.6	31.7	31.7	32.1	32.5	32.6	32.6
propene	14.7	14.5	14.7	14.7	14.4	14.2	13.7	13.8	14.4	14.8	14.1	14.2	13.1	14.1	14.3	14.7	14.2	14.4	13.1	14.1	14.3	14.7	14.2	14.4
1-butene	1.2	1.2	1.2	1.2	1.1	1.1	1.1	1.1	1.1	1.2	1.1	1.1	1.1	1.1	1.2	1.2	1.1	1.2	1.1	1.1	1.2	1.2	1.1	1.2
iso-butene	0.3	0.3	0.3	0.4	0.4	0.4	0.2	0.3	0.3	0.3	0.3	0.4	0.2	0.3	0.3	0.3	0.3	0.3	0.2	0.3	0.3	0.3	0.3	0.3
1.3-butadiene	6.2	6.2	6.2	6.1	5.8	5.4	6.0	5.9	5.9	5.9	5.7	5.7	6.1	6.1	6.2	6.2	5.9	5.7	6.1	6.1	6.2	6.2	5.9	5.7
C6−C8 aromatics	11.4	11.9	11.8	12.5	13.0	13.8	10.4	10.8	11.3	10.8	12.3	12.8	10.6	10.4	11.2	11.5	12.1	12.3	10.6	10.4	11.2	11.5	12.1	12.3
naphthalene	2.3	1.9	1.4	1.2	1.1	1.1	2.5	3.1	2.4	2.0	1.8	1.1	1.7	2.7	1.8	1.4	1.2	1.2	1.7	2.7	1.8	1.4	1.2	1.2
other PAHs	1.6	1.5	1.2	1.3	1.7	2.2	1.4	2.1	1.8	1.4	1.8	1.6	0.8	1.8	1.3	1.1	1.3	1.4	0.8	1.8	1.3	1.1	1.3	1.4

[a]HC-flow = 4.0 kg h^{-1}, steam dilution = 0.45 kg steam/kg feed, coil outlet temperature = 850° C, coil outlet pressure = 0.17 MPa; residence time = 0.3 s.

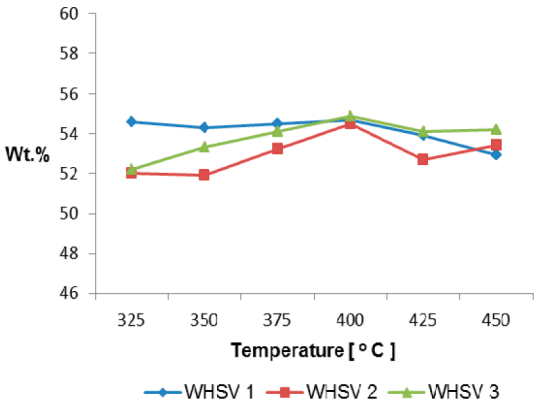

Figure 8. Simulated total yield of olefins obtained for steam cracking of hydrotreated DTO (organic phase) at different process conditions.

typical steam cracking conditions for all 18 experimental HDO DTO conditions. COILSIM1D is a single event microkinetic model that enables accurate and efficient modeling of the numerous reactions taking place in a steam cracking reactor.[40,41] The simulations have been carried out for the same reactor geometry[4] and using identical process conditions on the process gas side. The detailed conditions and reactor geometry can be found in the Supporting Information.

Overall, very high ethylene, propylene, and 1,3-butadiene yields were obtained in all 18 cases as represented in Table 4 . The maximal yield of ethylene is more than 32 wt % which is higher than what is achieved with a classical naphtha feedstock.[42] Also the high yields of propylene and 1,3 butadiene at these high severities are very attractive for a cracker because of their high value as building blocks for the chemical industry. Figure 8 shows that the simulated total light olefin yield from the hydrotreated DTO is higher at 400 °C irrespective of space time because in these cases the amount of paraffins in the hydrotreated DTO is higher and the DOD is higher as well. Paraffinic liquids are commonly considered very desirable feedstocks for steam cracking due to the high light olefin yields they tend to give.[35,4] Note that the remaining oxygen of the feed almost completely ends up forming CO and CO_2 according to the simulations. The latter is in line with the experimental work of Pyl et al.[43] and Herbinet et al.[44] The amount of CO and CO_2 produced from the hydrotreated DTO is directly related to degree of deoxygenation. At lower temperatures the DOD is higher and hence also the CO and CO_2 content present in the steam cracker product is lower. Another reason not to work with the HDO product obtained at higher HDO temperatures, next to mechanical issues due to the acidity, is the higher yield of invaluable fuel oil.

5. CONCLUSIONS

Catalytic upgrading of DTO over a commercial NiMo catalyst drastically reduced the oxygen content and produced a high paraffinic liquid hydrocarbon stream. The optimal conditions for maximal yield of paraffins were WHSV = 1 h^{-1} and T = 325−400 °C with maximum (~100%) DOD from the organic phase. Modest temperatures (<400 °C) are preferred because under these conditions oxygenates in DTO are converted by hydrodeoxygenation, hydrodecarboxylation/decarboxylation, and hydrodecarbonylation reactions. At higher temperatures nonselective deoxygenation and cracking mainly occurs, and more low value gaseous products are produced as well as (poly)aromatics. The catalyst maintained its activity as

demonstrated in a prolonged stability test of more than 32 h. Resulting liquid product has the potential to be used as feedstock for the production of olefins, and the simulated total olefin yield was more than 50% under typical steam cracking conditions.

■ ASSOCIATED CONTENT

Ⓢ Supporting Information

Details of GC × GC settings and the method used for the analysis; details of GC−MS and GC analysis; the detailed conditions and reactor geometry used for COILSIM1D. This material is available free of charge via the Internet at http://pubs.acs.org.

■ AUTHOR INFORMATION

Corresponding Author

*E-mail: Jinto.manjalyanthonykutty@vtt.fi. Tel.: +358207225721.

Notes

The authors declare no competing financial interest.

■ ACKNOWLEDGMENTS

Jinto Manjaly Anthonykutty acknowledges the financial support from VTT graduate school. The authors acknowledge Stora Enso for supporting this research and their vision on wood-based olefins. The authors also acknowledge Kiuru Jari and Juha Kokkonen for their help in analytics, in particular for interpreting GC−MS peaks.

■ NOMENCLATURE

HDO = hydrodeoxygenation
DTO = distilled tall oil
CTO = crude tall oil
AGO = atmospheric gas oil
WHSV = weight hourly space velocity
HDO−DTO = hydrodeoxygenated distilled tall oil
LHSV = liquid hourly space velocity
GC × GC = comprehensive 2-dimensional gas chromatograph
ToF-MS = time-of-flight mass spectrometer
FID = flame ionization detector
GC−MS = gas chromatography−mass spectrometric
FT-IR = Fourier transform-infrared spectroscopy
DOD = degree of deoxygenation
TMPAH = trimethylphenylammonium hydroxide
MPa = mega pascal
PAH = polyaromatic hydrocarbons

■ REFERENCES

(1) Elliott, C. D.; Hart, R. T.; Neuenschwander, G. G.; Rotness, J. L.; Zacher, H. A. Catalytic Hydroprocessing of Biomass Fast Pyrolysis Bio-oil to Produce Hydrocarbon Products. *Environ. Prog. Sustain. Energy* **2009**, *28* (3), 441−449.

(2) Sunde, K.; Brekke, A.; Solberg, B. Environmental Impacts and Costs of Hydrotreated Vegetable Oils, Transesterified Lipids and Woody BTL—A Review. *Energies* **2011**, *4* (6), 845−877.

(3) Gornay, J.; Coniglio, L.; Billaud, F.; Wild, G. Steam Cracking and Steam Reforming of Waste Cooking Oil in a Tubular Stainless Steel Reactor with Wall Effects. *Energy Fuels* **2009**, *23* (11), 5663−5676.

(4) Pyl, S. P.; Schietekat, C. M.; Reyniers, M. F.; Abhari, R.; Marin, G. B.; Van Geem, K. M. Biomass to Olefins: Cracking of Renewable Naphtha. *Chem. Eng. J.* **2011**, *176−177*, 178−187.

(5) Pyl, S. P.; Dijkmans, T.; Anthonykutty, J. M.; Reyniers, M. F.; Harlin, A.; Van Geem, K. M.; Marin, G. B. Wood-Derived Olefins by Steam Cracking of Hydrodeoxygenated Tall Oils. *Bioresour. Technol.* **2012**, *126*, 48−55.

(6) Press release, PepsiCo. 15.03.2011 http://www.pepsico.com/PressRelease/PepsiCo-Develops-Worlds-First-100-Percent-Plant-Based-Renewably-Sourced-PET-Bott03152011.html.

(7) Press release, Coca.Cola. 15.12,2011 http://www.Coca-colacompany.Com/media-center/press-releases/the-coca-cola-company-announces-partnerships-to-develop-commercial-solutions-for-plastic-bottles-made-entirely-from-plants.

(8) Coll, R.; Udas, S.; Jacoby, W. A. Conversion of the Rosin Acid Fraction of Crude Tall Oil into Fuels and Chemicals. *Energy Fuels* **2001**, *15*, 1166−1172.

(9) Sharma, R. K.; Bakhshi, N. N. Catalytic Conversion of Crude Tall Oil to Fuels and Chemicals over HZSM-5: Effect of Co-feeding Stream. *Fuel Process. Technol.* **1991**, *27*, 113−130.

(10) Furrer, R. M.; Bakhshi, N. N. Catalytic Conversion of Tall Oil to Chemicals and Gasoline Range Hydrocarbons. *Res. Thermochem. Biomass Convers.* **1988**, 956.

(11) Furimsky, E. Catalytic Hydrodeoxygenation. *Appl. Catal. A* **2000**, *199*, 147−190.

(12) Furimsky, E. Selection of Catalysts and Reactors for Hydroprocessing. *Appl. Catal. A* **1998**, *171*, 177−206.

(13) Sharma, R. K.; Bakhshi, N. N. Upgrading of Tall Oil to Fuels and Chemicals over HZSM-5 Catalyst Using Various Diluents. *Can. J. Chem. Eng.* **1991**, *69* (5), 1082−1086.

(14) Mikulec, J.; Kleinova, A.; Cvengros, J.; Joríkova, Ľ.; Banic, M. Catalytic Transformation of Tall Oil into Biocomponent of Diesel Fuel. *Int. J. Chem. Eng.* **2012**, DOI: 10.1155/2012/215258.

(15) Rozmysłowicz, B.; Mäki-Arvela, P.; Lestari, S.; Simakova, O. A.; Eränen, K.; Simakova, I. L.; Murzin, D. Y.; Salmi, T. O. Catalytic Deoxygenation of Tall Oil Fatty Acids Over a Palladium-Mesoporous Carbon Catalyst: A New Source of Biofuels. *Top. Catal.* **2010**, *53*, 1274−1277.

(16) Donnis, B.; Egeberg, R. G.; Blom, P.; Knudsen, K. G. Hydroprocessing of Bio-Oils and Oxygenates to Hydrocarbons. Understanding the Reaction Routes. *Top. Catal.* **2009**, *52* (3), 229−240.

(17) Guzman, A.; Torres, J. E.; Prada, L. P.; Nuñez, M. L. Hydroprocessing of Crude Palm Oil at Pilot Plant Scale. *Catal. Today* **2010**, *156* (1−2), 38−43.

(18) Mikulec, J.; Cvengros, J.; Joríkova, Ľ.; Banic, M. Kleinova, Second Generation Diesel Fuel from Renewable Sources. *J. Clean. Prod.* **2010**, *18*, 917−926.

(19) Kikhtyanin, O. V.; Rubanov, A. E.; Ayupov, A. B.; Echevsky, G. V. Hydroconversion of Sunflower Oil on Pd/SAPO-31 catalyst. *Fuel* **2010**, *89*, 3085−3096.

(20) Kubička, D.; Šimáček, P.; Žilková, N. Transformation of Vegetable Oils into Hydrocarbons over Mesoporous-Alumina-Supported CoMo Catalysts. *Top. Catal.* **2009**, *52* (1−2), 161−168.

(21) Clark, I. T.; Harris, E. E. Catalytic Cracking of Rosin. *J. Am. Chem. Soc.* **1952**, *74* (4), 1030−1032.

(22) Dutta, R. P.; Schobert, H. H. Hydrogenation/Dehydrogenation Reactions of Rosin. *Fundam. Studies Coal Liquefaction* **1993**, *38* (3), 1140−1146.

(23) Severson, R. F.; Schuller, W. H. The Thermal Behavior of Some Resin Acids at 400−500 °C. *Can. J. Chem.* **1972**, *50*, 2224.

(24) Şenol, O. I.; Ryymin, E.-M.; Viljava, T.-R.; Krause, A. O. I. Effect of hydrogen sulphide on the hydrodeoxygenation or aromatic and aliphatic oxygenates on sulphided catalysts. *J. Mol. Catal. A* **2007**, *227* (1−2), 107−112.

(25) Knuuttila, P.; Nousiainen, J.; Rissanen, A. Process and Apparatus for Producing Hydrocarbons from Feedstocks Comprising Tall Oil and Terpene-Compounds. WO2011148046 (A1) 2011, 26 pp.

(26) Van Geem, K. M.; J. Ongenae, J. L.; Brix, J. V.; Marini, G. B. Ultratrace Quantitative Analysis of Catalyst Poisoners Using a Dedicated GC−MS Analyzer. *LC−GC Eur.* **2012**, *25* (4), 172−+.

(27) Reuss, G.; Disteldorf, W.; Gamer, A. O.; Hilt, A. Formaldehyde. Ullmann's Encyclopedia of Industrial Chemistry: Wiley-VCH Verlag GmbH & Co.: Weinheim, Germany, 2000.
(28) Dethrow, M. Methanol in Cracking Furnaces. Paper presented at Annual Ethylene Producers Conference; New Orleans, LA, 1996.
(29) Van Geem, K. M.; Anthonykutty, J. M.; Pyl, S. P.; Harlin, A.; Marin, G. B.Production of bioethylene: Alternatives for green chemicals and polymers. AIChE Spring Meeting and 8th Global Congress on Process Safety, 12AIChE, Houston, Texas, 2012.
(30) Mortensen, P. M.; Grunwaldt, J.-D.; Jensen, P. A.; Knudsen, K. G.; Jensen, A. D. A review of catalytic upgrading of bio-oil to engine fuels. *Appl. Catal. A* **2011**, *407*, 1−19.
(31) Venderbosch1, R. H.; Ardiyanti, A. R.; Wildschut, J.; Oasmaa, A.; Heeres, H. J. Stabilization of biomass-derived pyrolysis oils. *J. Chem. Technol. Biotechnol.* **2010**, *85*, 674−686.
(32) Satyarthi, J. K.; Chiranjeevi, T.; Gokak, D. T.; Viswanathan, P. S. An overview of catalytic conversion of vegetable oils/fats into middle distillates. *Catal. Sci. Technol.* **2013**, *3*, 70−80.
(33) Kubička, D.; Bejblová, M.; Vlk, J. Conversion of Vegetable Oils into Hydrocarbons over CoMo/MCM-41 Catalysts. *Top. Catal.* **2010**, *53*, 168−178.
(34) Kubička, D.; Kaluza, L. Deoxygenation of Vegetable Oils over Sulfided Ni, Mo, and NiMo Catalysts. *Appl. Catal. A* **2010**, *372*, 199−208.
(35) Huber, G. W.; O'Connor, P.; Corma, A. Processing Biomass in Conventional Oil Refineries: Production of High Quality Diesel by Hydrotreating Vegetable Oils in Heavy Vacuum Oil Mixtures. *Appl. Catal.* **2007**, *329*, 120−129.
(36) Monnier, J.; Sulimma, H.; Dalai, A.; Caravaggio, G. Hydrodeoxygenation of oleic acid and canola oil over alumina-supported metal nitrides. *Appl. Catal. A* **2010**, *382*, 176−180.
(37) Kubičková, I.; Kubička, D. Utilization of Triglycerides and Related Feedstocks for Production of Clean Hydrocarbon Fuels and Petrochemicals: A Review. *Waste Biomass Valorization* **2010**, *1* (3), 293−308.
(38) Bernas, A.; Salmi, T.; Murzin, Yu, D.; Mikkola, J.; Rintola, M. Catalytic Transformation of Abietic Acid to Hydrocarbons. *Top Catal.* **2012**, *55*, 673−679.
(39) Šimáčeka, P.; Kubička, D.; Kubičková, I.; Homola, F.; Pospíšila, M.; Chudoba, J. Premium Quality Renewable Diesel Fuel by Hydroprocessing of Sunflower Oil. *Fuel* **2011**, *90*, 2473−2479.
(40) Van Geem, K. M.; Reyniers, M. F.; Marin, G. B. Challenges of Modeling Steam Cracking of Heavy Feedstocks. *Oil Gas Sci. Technol.—Revue de l'institut francais du petrole* **2008**, *63* (1), 79−94.
(41) Sabbe, M. K.; Van Geem, K. M.; Reyniers, M. F.; Marin, G. B. First Principle-Based Simulation of Ethane Steam Cracking. *AIChE J.* **2011**, *57* (2), 482−496.
(42) Pyl, S. P.; Van Geem, K. M.; Reyniers, M. F.; Marin, G. B. Molecular Reconstruction of Complex Hydrocarbon Mixtures: An Application of Principal Component Analysis. *AIChE J.* **2009**, *56* (12), 3174−3188.
(43) Pyl, S. P.; Van Geem, K. M.; Puimege, P.; Sabbe, M. K.; Reyniers, M. F.; Marin, G. B. A comprehensive study of methyl decanoate pyrolysis. *Energy* **2012**, *43* (1), 146−160.
(44) Herbinet, O.; Glaude, P. A.; Warth, V.; Battin-Leclerc, F. Experimental and modeling study of the thermal decomposition of methyl decanoate. *Combust. Flame* **2011**, *158* (7), 1288−1300.